Journal of Catalysis 342 (2016) 138–150

Contents lists available at ScienceDirect

Journal of Catalysis

journal homepage: www.elsevier.com/locate/jcat

Development of reusable palladium catalysts supported on hydrogen titanate nanotubes for the Heck reaction

Mark E. Martínez-Klimov [a], Patricia Hernandez-Hipólito [a], Tatiana E. Klimova [b,*], Dora A. Solís-Casados [c], Marcos Martínez-García [a]

[a] Instituto de Química, Universidad Nacional Autónoma de México, Ciudad Universitaria, Circuito Exterior, Coyoacán, Ciudad de México 04510, Mexico
[b] Facultad de Química, Universidad Nacional Autónoma de México, Ciudad Universitaria, Coyoacán, Ciudad de México 04510, Mexico
[c] Centro Conjunto de Investigación en Química Sustentable, UAEM-UNAM, Km 14.5, Carretera Toluca-Atlacomulco, San Cayetano, Toluca, Estado de México 50200, Mexico

ARTICLE INFO

Article history:
Received 17 May 2016
Revised 23 July 2016
Accepted 25 July 2016

Keywords:
Palladium catalysts
Hydrogen titanate nanotubes
Cross-coupling Heck reaction
Catalytic activity
Deactivation

ABSTRACT

Palladium catalysts supported on hydrogen titanate nanotubes were prepared by adsorption of palladium (II) acetate from dichloromethane solutions. At low $Pd(OAc)_2$ loadings (up to 5 wt.%), the catalysts contained only highly dispersed chemisorbed Pd^0 and $Pd^{2+}O$ species (XPS). Characteristic signals of Pd $(OAc)_2$ were not detected in these catalysts by FT-IR, FT-Raman, of XPS, indicating decomposition of the precursor salt due to the strong metal–support interaction. An increase in the palladium loading resulted in an increase in the proportion of Pd^0 species and the appearance of some supported Pd $(AcO)_2$ (XPS). In the sample with the highest palladium loading (8.84 wt.% of $Pd(OAc)_2$), formation of small (~1.2–2.4 nm) palladium-containing clusters was detected on the support surface by HRTEM. Catalytic activity was tested in the Heck reaction between 4-bromobenzaldehyde or 4-bromostyrene and styrene. Only the E-isomers of the corresponding cross-coupled products were obtained. The activity and TON numbers of the supported Pd catalysts were higher than those of the palladium(II) acetate under homogeneous catalysis conditions. Strong palladium–support interaction resulted in the generation of catalytically active Pd(0) species without additional reduction pretreatment of the catalyst. The possibility of reuse of the same catalysts in several catalytic cycles was tested. It was found that both the Pd loading in the catalysts and the amount of water in the support have a strong influence on the catalyst's deactivation. A catalyst with stable activity, able to be recycled at least five times, was prepared with Pd loading of 5 wt.% of $Pd(AcO)_2$ using titanate nanotubes calcined at 350 °C for 2 h prior to the preparation of the catalyst.

1. Introduction

Carbon–carbon bond formation is a general aim in organic chemistry synthesis catalyzed by transition metals yielding valuable fine chemicals. The Heck coupling reaction is an effective method for the C–C cross-coupling of aryl halides with aryl or alkenyl compounds, leading to a variety of alkenes with great pharmaceutical and industrial value [1–3]. The growing demand for fine chemicals in the industries and increasingly stringent ecological standards require development of new technologies for cross-coupling reactions catalyzed by transition metal catalysts in order to provide convenient synthetic routes for regio- and stereodefined systems [4,5]. Different palladium catalysts, homogeneous and heterogeneous, have been widely used for the cross-coupling Heck reaction, giving good results. Nevertheless, homogeneous Heck catalysis has some drawbacks, such as difficulty of catalyst separation and reuse after the reaction, as well as facile deactivation leading to limited catalyst lifetime. Because of this, in the past few years, several attempts have been made to prepare active, stable, and easy-to-handle and -separate palladium catalysts. Palladium catalysts supported on different materials (carbon [5], metal oxides [6], layered clays [7], zeolites [8], mesoporous molecular sieves [9], carbon nanotubes [10], etc.) or encapsulated in large organic structures (dendrimers [11], block copolymer micelles [12], etc.) have attracted much attention. The interest in them is due principally to the fact that immobilization of Pd nanoparticles on the surface of a solid material or inside an organic matrix makes it possible to stabilize catalytically active well-dispersed metal species and prevent their sintering. In [9], Pd-TMS11 catalysts with high Pd dispersion (25–32%) were prepared by the vapor grafting of a volatile organometallic complex [Pd(η-C_5H_5)-(η^3-C_3H_5)] onto the surface of

* Corresponding author. Fax: +52 55 56225371.
E-mail address: klimova@unam.mx (T.E. Klimova).

http://dx.doi.org/10.1016/j.jcat.2016.07.019
0021-9517/

Nb-MCM-41 material previously degassed at 600 °C, followed by the reduction of the catalyst in a stream of hydrogen at 350 °C for 3 h. These catalysts showed high catalytic activity (TON numbers between 1000 and 5000) for the cross-coupling Heck reaction of n-butyl acrylate with activated aryl substrate. However, the Pd-TMS11 catalyst, recovered after the catalytic test, showed some agglomeration of palladium and partial structural damage of the Nb-MCM-41 support material [9]. In [10], poly(lactic acid) grafted carbon nanotubes (*f*-CNTs) were used as a platform for in situ deposition of Pd nanoparticles. The obtained catalysts were found to be effective in the promotion of the Heck cross-coupling reaction between aryl halides and n-butyl acrylate. The recycled *f*-CNTs-Pd nanocatalyst showed stable activity in another three reaction cycles. However, up to now, the search for new heterogeneous catalysts with well-dispersed and stable supported Pd species remains an incomplete task.

In the present work, palladium catalysts supported on hydrogen titanate nanotubes were prepared and tested in the cross-coupling Heck reaction. Hydrogen titanate nanotubes are a novel and intensively studied material that has attracted much attention in the past decade because of its unique textural and physicochemical properties [13–16]. This material found a variety of applications, including catalysis [17,18] and photocatalysis [19,20]. Titanate nanotubes have high specific surface area (~200–400 m^2/g), internal tube diameter between 3 and ca. 10 nm, open mesoporous morphology [21,22], and an absence of micropores that facilitate transport of reagents and products during a catalytic reaction. The high cation exchange capacity [14,23] of hydrogen titanate nanotubes should enable high loading of an active catalyst with even distribution and high dispersion. The semiconducting properties of titanate nanotubes [24,25] may result in a strong electronic interaction between the support and a catalyst, which could be beneficial for some catalytic reactions. Palladium catalysts supported on titanate nanotubes have already been prepared by an ion-exchange technique [23,26], incipient wetness impregnation [27], and photodeposition [28] and by hydrothermal synthesis of titanate nanotubes with the simultaneous addition of a $PdCl_2$ precursor [29]. In all these cases, water was used as a solvent. Palladium catalysts with different characteristics were obtained depending on the preparation method used and the palladium loading. Here we report on the synthesis of palladium catalysts supported on hydrogen titanate nanotubes by adsorption of Pd (II) acetate from a nonaqueous solvent (dichloromethane). We selected this method of preparation because of its simplicity and the possibility of deposition of palladium species only by interaction with the support. Catalysts were characterized and tested in the Heck reactions between activated aryl substrates (4-bromobenzaldehyde or 4-bromostyrene) and styrene.

2. Experimental

2.1. Support and catalyst preparation

Sodium titanate nanotubes were synthesized by an alkali hydrothermal treatment following a procedure reported by Kasuga et al. [13,30]. Commercial titanium dioxide (anatase, Aldrich, 54 m^2/g) was used as the TiO_2 source. In each synthesis, 10 g of TiO_2 was mixed with 150 ml of a 10 M alkali solution, followed by hydrothermal treatment in a Teflon-lined autoclave at 140 °C for 20 h under constant magnetic stirring. After the hydrothermal reaction, the white powder of sodium titanate nanotubes (NaNT) was filtered in vacuum, thoroughly washed with deionized water to eliminate the excess of nonreacted NaOH, and dried at 120 °C for 12 h. To decrease the sodium content, the dry NaNT was slurried into a 0.1 M HCl solution for 2 h (100 mL of solution per 2 g of NaNT), filtered, washed with deionized water, and dried again at 120 °C for 12 h. This procedure resulted in the formation of hydrogen titanate nanotubes with low content of residual sodium (below 0.1 wt.%), which will be denoted hereafter as NT. Part of the synthesized NT material was calcined at 350 °C for 2 h (NTc sample). Palladium catalysts supported on the synthesized NT or NTc were prepared by adsorption of Pd(II) acetate ($Pd(OAc)_2$) from dichloromethane solutions. Briefly, 1 g of the support was slurried in 30 mL of CH_2Cl_2 solution of $Pd(OAc)_2$ for 8 h at room temperature. After the first hour of this treatment, the white powder of the support changed color to light brown, whose intensity depended on the initial concentration of $Pd(OAc)_2$. The catalysts were filtered, washed with a small amount of CH_2Cl_2, and dried at room temperature and then at 120 °C for 12 h. The remaining solutions were analyzed by atomic absorption spectroscopy (Perkin–Elmer) to determine the quantity of adsorbed palladium. In addition, palladium loading in the dried catalysts was determined by SEM-EDX, giving good correlation between both techniques. Four catalysts with nominal $Pd(OAc)_2$ loadings between 2.5 and 10 wt.% were prepared using the NT support and two catalysts using the NTc material. Hereinafter, the prepared catalysts are designated as Pd(*x*)/NT or Pd(*x*)/NTc, where *x* is the theoretical wt.% of $Pd(OAc)_2$ in the catalyst.

2.2. Catalyst characterization

Obtained hydrogen titanate nanotubes (NT and NTc) and catalysts were characterized by N_2 physisorption, X-ray powder diffraction (XRD), scanning electron microscopy (SEM-EDX), transmission electron microscopy (TEM), thermogravimetric analysis (TGA), and FT-IR, FT-Raman, and X-ray photoelectron spectroscopy (XPS). Nitrogen adsorption–desorption isotherms were measured with a Micromeritics ASAP 2020 automatic analyzer at liquid N_2 temperature. Prior to the experiments, the samples were degassed ($p < 10^{-1}$ Pa) at 250 °C for 6 h. Specific surface areas (S_{BET}) were calculated by the BET method, the total pore volume (V_p) was determined by nitrogen adsorption at a relative pressure of 0.98, and pore diameters (D_P) and pore size distributions were obtained from the adsorption isotherms by the BJH method. The X-ray powder diffraction patterns of the synthesized samples were recorded at room temperature from 3 to 80° (2θ) on a Bruker D8 Advance diffractometer, using Cu Kα radiation ($\lambda = 1.5406$ Å) and a goniometer speed of 1° (2θ) min^{-1}. The chemical composition of the synthesized materials was determined by SEM-EDX using a JEOL 5900 LV microscope with OXFORD ISIS equipment. High-resolution transmission electron microscopy (HRTEM) images were recorded with a JEOL 2010 microscope operating at 200 kV (resolving power 1.9 Å). The solids were ultrasonically dispersed in heptane and the suspension was collected on carbon-coated grids. HRTEM pictures were taken from different parts of the same sample dispersed on the microscope grid. TGA analysis was used to determine the amount of chemisorbed water in the synthesized materials. TGA experiments were performed on a Mettler-Toledo TGA/SDTA 851^e in dry air flow (50 ml/min) in the temperature range between 25 and 1000 °C with a heating rate of 10 °C/min. FT-IR spectra were recorded on a Varian 640-IR spectrometer equipped with a PIKE accessory. Micro-Raman spectra of the catalysts were obtained using an HR LabRam 800 system equipped with an Olympus BX40 confocal microscope. A Nd:YAG laser beam (532 nm) was focused by a 50× microscope objective onto an ≈1 μm diameter on the sample surface. The laser power at the sample was regulated by a neutral density filter (OD = 1) to prevent sample heating and structural changes induced in the sample. A cooled CCD camera was used to record the spectra, usually averaged for 100 accumulations in order to improve the signal-to-noise ratio. All spectra were calibrated using the 521 cm^{-1} line of

a silicon wafer. XPS measurements were performed with a JEOL JPS-9200 instrument equipped with a Mg Kα radiation source (1253.6 eV). The spectrometer was operated at a pass energy of 10 eV with an X-ray power of 300 W. The base pressure in the analyzing chamber was maintained on the order of 1×10^{-8} mbar. The binding energy was determined using the carbon C (1*s*) line as a reference with a binding energy of 284 eV. Quantification and deconvolution were performed using the Gaussian functions of the Origin 8.1 software.

2.3. General procedure for the Heck reaction

Styrene, 4-bromobenzaldehyde, 4-bromostyrene, triethylamine, tri-(o-tolyl)phosphine (TOP), and N,N-dimethylformamide were obtained from Sigma-Aldrich. Reactions were performed in a 250-mL three-necked glass flask under reflux. In a typical experiment, the flask was charged with 4-bromobenzaldehyde or 4-bromostyrene (13.5 mmol), styrene (13.5 mmol), triethylamine (10 mL), TOP (1.64 mmol), and N,N-dimethylformamide (25 mL). The reaction mixture was heated to 150 °C and varied amounts of the palladium catalyst (Pd(*x*)/NT or Pd(*x*)/NTc) was added. The reaction was monitored by TLC. After completion of the reaction, the catalysts were recovered by filtration and dried in air at room temperature for 12 h and the reaction mixture was concentrated under reduced pressure. Purification of the E/Z-isomers was carried out by column chromatography with silica gel and a hexane/ethyl acetate (8:2) solvent mixture, giving analytically pure products. The obtained reaction products were characterized by ^{1}H and ^{13}C NMR, IR, mass spectrometry, and elemental analysis (Fig. S6 and product characterization in the Supporting Information). ^{1}H and ^{13}C NMR spectra were recorded on a Varian Unity 300 MHz with tetramethylsilane (TMS) as an internal reference. Infrared (IR) spectra were measured on a spectrophotometer FT-IR MAGNA 700. Mass spectra were taken on a JEOL JMS AX505 HA instrument. Turnover numbers (TON) were calculated as mol of obtained product per mol of Pd, disregarding the oxidation state of palladium species.

3. Results

3.1. Support and fresh catalysts characterization

Fig. 1 shows a TEM micrograph of the as-synthesized NaNT material and the same material after washing with diluted hydrochloric acid, during which Na^{+} cations were exchanged with H^{+} resulting in the NT support. In both images, randomly distributed open-ended nanotubular structures with 3–5 layered walls can be observed. They are not always symmetric, with small dispersion in inner and outer diameters and of different lengths. The external diameters of the nanotubes were around 10–12 nm, the internal pore size about 6–7 nm, and the lengths of the tubes ranged from 50 to 200 nm. Observed layered structures of the tube walls had interlayer spaces of ~0.8 nm. This result is in line with previous reports [13,30,31] and confirms successful preparation of sodium and hydrogen titanate nanotubes.

The X-ray diffraction pattern of the synthesized NT material is shown in Fig. S1 in the Supporting Information. In the diffractogram, three main diffraction peaks were observed at 11.2, 24.4, and 48.4° (2θ). These reflections are typical of the monoclinic layered hydrogen trititanate phase $H_2Ti_3O_7$ (JCPDS-ICDD Card 47-0561) [31], which forms the curved nanotubular walls, and can be indexed to its (200), (110), and (020) crystal planes, respectively. The signal at 11.2° (2θ) is attributed to the interlayer distance of hydrogen trititanate and is equal to 0.79 nm, which is in good agreement with the HRTEM results described above. The broadness of all observed diffraction signals indicates the poorly crystalline nature of the synthesized titania nanotubes, which is in line with previous reports for similar materials [32,33]. No reflections attributable to TiO_2 anatase used as a precursor were detected, indicating that it was transformed into trititanate nanotubes.

Nitrogen physisorption showed that the NT support had attractive textural characteristics: 260 m^2/g specific surface area and 0.62 cm^3/g total pore volume (Table 1). The corresponding N_2 adsorption–desorption isotherm and pore volume distribution are shown in Fig. S2 in the Supporting Information. The isotherm was of type IV, according to the IUPAC classification [34], with a noticeable hysteresis loop, which confirms the presence of meso- and macropores. Pore size distribution presented a main pore contribution at 7.3 nm, which corresponds well to the internal pore size of titanate nanotubes observed by HRTEM, and two lower-intensity signals at 3 and about 50 nm. The pores with a diameter of 3 nm can indicate the presence of a small proportion of titanate nanotubes with this internal size, whereas larger pores can be attributed to the voids in the aggregation of the nanotubes [35].

Palladium catalysts supported on the above-described NT support were prepared by adsorption of $Pd(OAc)_2$ from dichloromethane solution at room temperature (25 °C). The corresponding adsorption isotherm is shown in Fig. 2. It can be seen that at low Pd loadings, all palladium species are adsorbed onto the support surface, the residual concentration of $Pd(OAc)_2$ in the solution being less than 0.001 M (part I of the adsorption

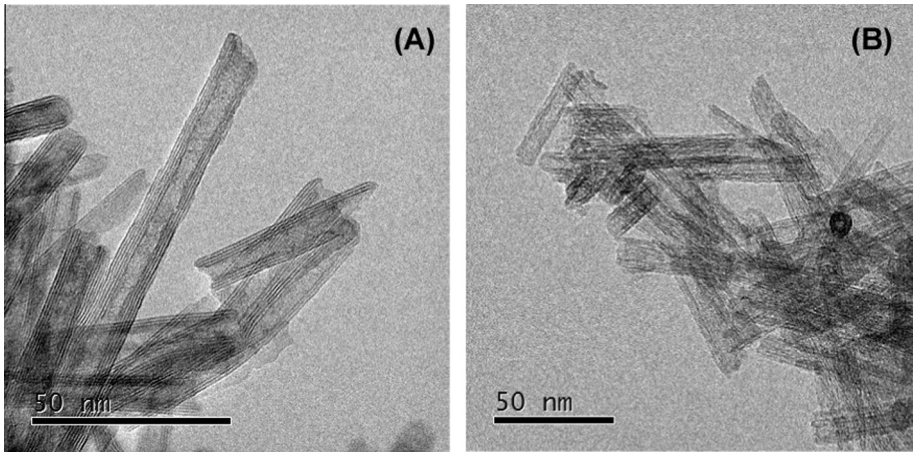

Fig. 1. HRTEM micrographs of as-synthesized NaNT (A) and NT (B) supports. Nanotubular structures of both materials shown can be seen.

Table 1
Chemical composition and textural characteristics of NT and NTc supports and prepared palladium catalysts.

Sample	Theoretical loading	Real Pd loading[a]		Textural characteristics[b]		
	$Pd(OAc)_2$ (wt.%)	$Pd(OAc)_2$ (wt.%)	Atoms Pd/nm^2	S_{BET} (m^2/g)	V_P (cm^3/g)	D_P (nm)
NT support	–	–	–	260	0.62	7.3
Pd(2.5)/NT	2.5	2.54	0.26	258	0.61	7.3
Pd(5.0)/NT	5.0	5.01	0.53	252	0.58	7.3
Pd(7.5)/NT	7.5	7.43	0.82	244	0.57	7.3
Pd(10)/NT	10.0	8.84	0.96	246	0.58	7.3
NTc support	–	–	–	269	0.72	8.9
Pd(5.0)/NTc	5.0	4.99	0.53	253	0.66	8.9
Pd(10)/NTc	10.0	8.57	0.94	245	0.65	8.8

[a] Determined by SEM-EDX.
[b] S_{BET}, specific surface area calculated by the BET method; V_P, total pore volume; D_P, pore diameter corresponding to the maximum of the pore size distribution calculated from the desorption isotherm by the BJH method.

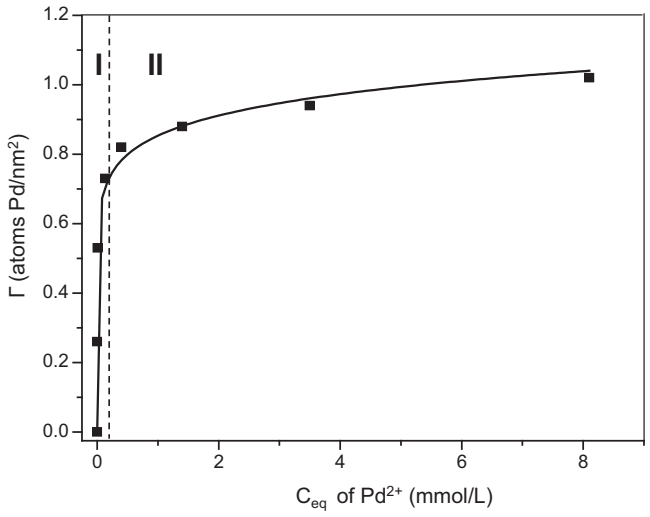

Fig. 2. Isotherm of adsorption of palladium (II) acetate on hydrogen titanate nanotubes in dichloromethane solutions at 25 °C. Part I of the isotherm corresponds to irreversible adsorption of Pd species, whereas Part II corresponds to reversible adsorption.

isotherm). In this part of the isotherm, Pd adsorption is irreversible and seems to be chemical. On the other hand, an increase in the Pd $(OAc)_2$ concentration (part II of the isotherm) resulted in a further increase in the amount of adsorbed palladium and the appearance of some residual Pd^{2+} species in the solution. In this second part of the isotherm, equilibrium is established between Pd^{2+} species in the solution and the adsorbed ones, which evidences the presence of some Pd species reversibly adsorbed on the NT surface, in addition to the chemisorbed ones. The above observation indicates the possibility of different types of adsorbed Pd species in the first and second parts of the isotherm. It is worth mentioning that previously, isotherms of similar shape were obtained for the adsorption of Pd^{2+}, Ru^{3+}, and Au^{3+} species from aqueous solutions onto titanate nanotubes [23,26]. The first part of the isotherms was attributed to the ion exchange of metal cations from solution with protons of the hydrogen titanate nanotubes. In the present work, we used Pd(II) acetate as the palladium source and a nonaqueous solvent (dichloromethane). Since dichloromethane is a polar solvent, the possibility of some ion exchange of Pd^{2+} species from the solution with protons of the support cannot be completely excluded. In addition, irreversible adsorption of Pd species in the first part of the isotherm may be due to strong palladium–support interaction leading to the appearance of some kind of chemisorbed Pd species, whereas in the second part of the isotherm, in addition to the chemisorbed Pd species, some physically adsorbed Pd appeared. These results suggest the possibility of coexistence of different types of Pd species adsorbed on the NT surface and that their relative proportions can change depending on the palladium loading.

For further characterization and catalytic activity evaluation, we selected four Pd(x)/NT catalysts with nominal $Pd(OAc)_2$ loadings of 2.5, 5.0, 7.5, and 10 wt.%. These freshly prepared samples are shown in Fig. 3. After palladium acetate adsorption, the white NT support changed color to light brown, the color becoming more intense with increasing Pd content.

Table 1 shows the chemical composition of the prepared catalysts determined by SEM-EDX analysis and their textural characteristics. It can be observed that, as expected, the amount of palladium in the catalysts was close to the theoretically expected value at low Pd loadings (up to 5 wt.% of $Pd(OAc)_2$), whereas at higher loadings the real amount of Pd in the catalysts was smaller, since some residual Pd species remained in the solution. For example, the Pd(10)/NT catalyst had 8.84 wt.% of palladium as $Pd(OAc)_2$ instead of the nominal 10 wt.% loading. Regarding textural characteristics of the catalysts, adsorption of Pd(II) acetate almost did not affect the textural characteristics of the NT support. Only a slight decrease in the surface area and total pore volume was observed after Pd incorporation, which can be attributed to an increase in the materials' density due to the adsorption of the $Pd(OAc)_2$ precursor. A detailed analysis of the N_2 adsorption–desorption isotherms and pore volume distributions of the catalysts (Fig. S2 in the Supporting Information) showed that the adsorption of Pd did not produce noticeable modifications in the characteristic shape of the N_2 adsorption–desorption isotherm of the NT support, nor in its pore structure. Pore diameter maintained the same value

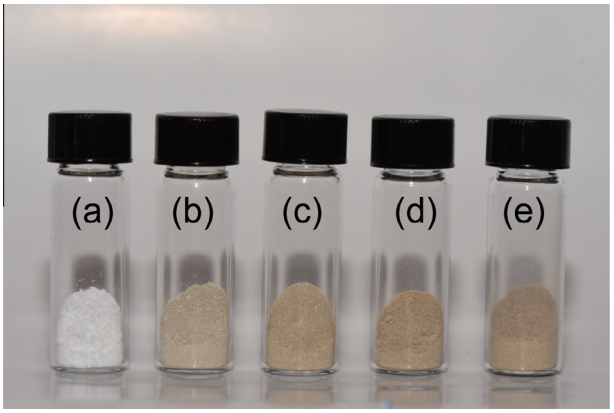

Fig. 3. NT support (a) and freshly prepared palladium catalysts: (b) Pd(2.5)/NT, (c) Pd(5.0)/NT, (d) Pd(7.5)/NT, and (e) Pd(10)/NT. White color of the NT support changed to light brown after adsorption of $Pd(OAc)_2$.

(7.3 nm) in all Pd(x)/NT catalysts as in the corresponding NT support. X-ray diffraction patterns of the Pd(x)/NT catalysts (Fig. S1 in the Supporting Information) were similar to that of the NT support; only the reflections characteristic of the hydrogen trititanate phase $H_2Ti_3O_7$ (JCPDS-ICDD Card 47-0561) of the support were observed. No reflections attributable to any Pd(II) or Pd(0) crystalline phase were detected, indicating good dispersion of the deposited Pd species.

Further insight into the palladium dispersion in the prepared catalysts was made by scanning electron microscopy (SEM-EDX) and high-resolution transmission electron microscopy (HRTEM) studies. Results obtained by SEM for the Pd(2.5)/NT catalyst are shown in Fig. 4, whereas palladium maps of other catalysts can be consulted in Fig. S3 in the Supporting Information. This study also confirmed that palladium was highly dispersed and homogeneously distributed over the surface of the NT support.

Characterization of the prepared palladium catalysts by HRTEM did not allow us to observe any kind of palladium species in the Pd (2.5)/NT, Pd(5.0)/NT, and Pd(7.5)/NT catalysts, which may be due to their very high dispersion. Only in the case of the Pd(10)/NT catalyst with the highest palladium loading were very small (~1.2–2.4 nm) Pd-containing clusters observed (Fig. 5).

Summarizing all the above characterization results, it can be stated that palladium catalysts with well-dispersed palladium species were prepared by the adsorption method used in the present work. In addition, it was assumed that different types of adsorbed species (chemisorbed and physisorbed ones) could be formed. Namely, at low Pd loadings, chemisorbed species were predominant, whereas at high metal loadings, some less strongly adsorbed species appeared (part II of the $Pd(OAc)_2$ adsorption isotherm). Probably the latter are those that were observed as small palladium-containing clusters by HRTEM. However, from all the above results, it was not clear if Pd(II) acetate was adsorbed intact onto the NT surface or if it suffered some transformations. In order to answer this question, FT-IR, FT-Raman, and XPS characterization of the prepared catalysts was performed.

Infrared spectra of the NT support and four Pd(x)/NT catalysts with different Pd loadings are shown in Fig. S4A in the Supporting Information. In the IR spectrum of the NT support, three main bands were observed. The first broad band in the range 3200–3500 cm^{-1} can be assigned to the stretching vibrations of adsorbed water and Ti–OH surface hydroxyl groups, ν(OH) [36]. The high intensity of this band can be attributed to high water content in the NT support, which can vary between 17 and 20 wt.% [36]. Another band was observed at 1632 cm^{-1}, which can be ascribed to the molecular water bending mode [37]. The last intense band, from about 1000 to 400 cm^{-1}, is generally related to the Ti–O and Ti–O–Ti skeletal frequency region. In the FT-IR spectra of all Pd catalysts, the above-mentioned characteristic vibrations of the NT support were observed, and in addition some new bands

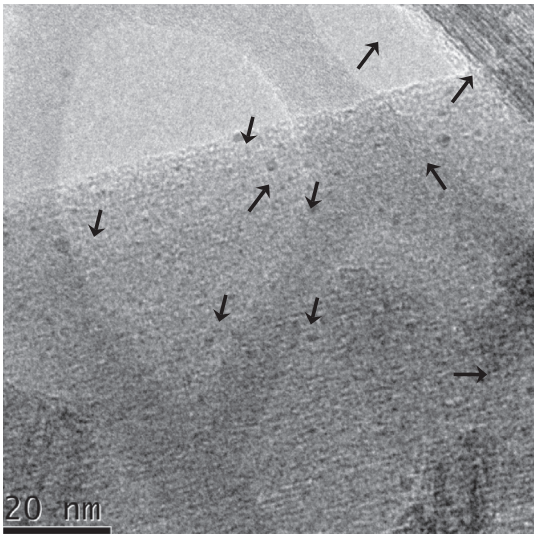

Fig. 5. HRTEM micrograph of fresh Pd(10)/TNT catalyst. Pd-containing clusters are indicated with arrows.

appeared between 1600 and 1350 cm^{-1}, which correspond to different vibration modes of the acetate group. Amplification of the region 1900–1100 cm^{-1} is shown in Fig. 6A. There are three vibrations for the acetate ligand in this region: asymmetric and symmetric stretching vibrations of the carboxylate ($\nu(COO)_{asym}$ and $\nu(COO)_{sym}$, respectively) and deformation vibrations for the methyl group ($\delta(CH_3)_{sym}$). Since the acetate group can exist in different coordination modes (bridging, bidentate, and monodentate) [38], the exact assignment of bands for the carboxylate stretching vibrations in acetate complexes sometimes is difficult. For comparison purposes, the spectra of solid Pd(II) acetate and $Pd(OAc)_2$ dissolved in dichloromethane were also recorded (Fig. 6B).

The FT-IR spectrum of solid $Pd(OAc)_2$, used as a palladium source, is shown in Fig. 6B (spectrum a). It is well known that Pd (II) acetate in the crystalline state exists as a trimer, $Pd_3(CH_3COO)_6$, with all acetate groups in bridging coordination (each acetate group forms a symmetrical bridge between two Pd atoms) [38]. The FT-IR spectrum obtained for this compound showed three bands located at 1595, 1416, and 1350 cm^{-1}. According to the literature [38–40], the first band at 1595 cm^{-1} is assigned to the asymmetric stretching vibrations $\nu(COO)_{asym}$, whereas the second band, with a maximum at 1416 cm^{-1}, corresponds to $\nu(COO)_{sym}$ with a contribution from $\delta(CH_3)_{sym}$ (~1430 cm^{-1}). A less intense band at 1350 cm^{-1} is assigned to the symmetric scissoring vibration of the acetate methyl group. The frequency of asymmetric and symmetric stretching vibrations depends on the coordination of the acetate group and on the nature of the metallic atom. There-

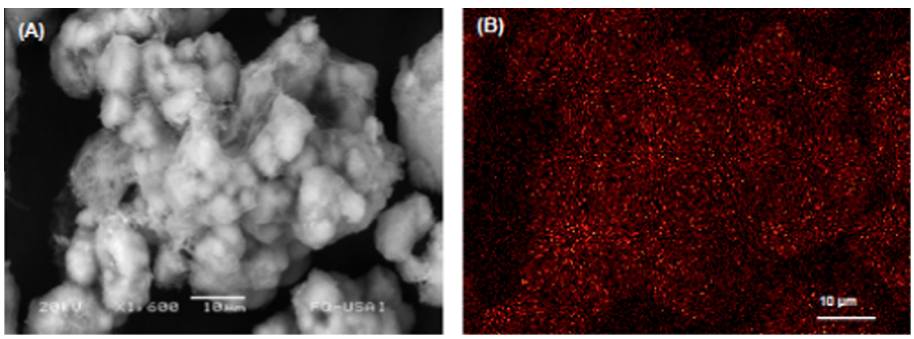

Fig. 4. SEM image of Pd(2.5)/NT catalyst (A) and corresponding palladium map (B). Homogeneous distribution of palladium on the support can be observed.

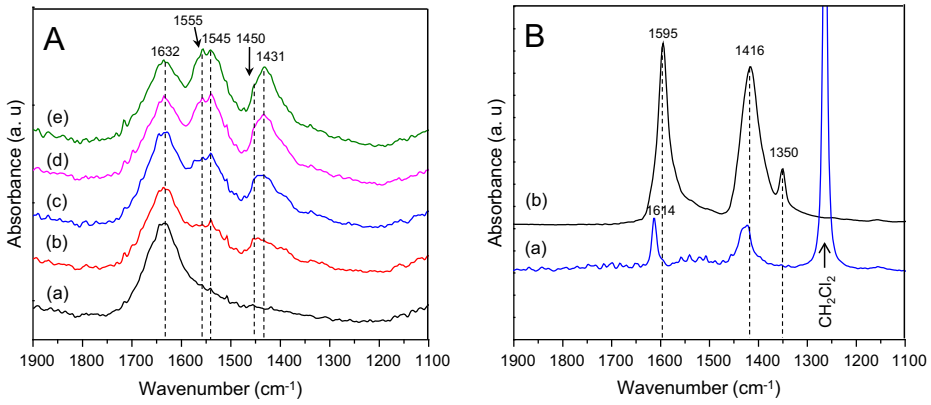

Fig. 6. (A) IR spectra of (a) NT support, (b) Pd(2.5)/NT, (c) Pd(5.0)/NT, (d) Pd(7.5)/NT, and (e) Pd(10)/NT. (B) Some reference IR spectra: (a) $Pd(OAc)_2$ solution in dichloromethane and (b) $Pd(OAc)_2$ trimer crystal.

fore, the differences (Δ_ν) in the wavenumbers of carboxyl asymmetric and symmetric stretch modes $\Delta_\nu = \nu(COO)_{asym} - \nu(COO)_{sym}$ help in the identification of the coordination mode of acetates. Thus, for the solid $Pd(OAc)_2$, the value of Δ_ν was equal to 179 cm^{-1}, which is in line with the previously reported value of 184 cm^{-1} corresponding to acetate bridging two Pd atoms [38]. When $Pd(OAc)_2$ was dissolved in dichloromethane, only a slight shift of the $\nu(COO)_{asym}$ and $\nu(COO)_{sym}$ signals to higher wavenumbers was observed, probably because of solvation, indicating that a trimeric Pd(II) acetate structure was maintained intact in the CH_2Cl_2 solution. Regarding the spectra of Pd catalysts (Fig. 6A), vibrations of the acetate group were observed at positions other than those of the $Pd(OAc)_2$ trimer, namely at about 1550 cm^{-1} ($\nu(COO)_{asym}$) and 1450-1430 cm^{-1} ($\nu(COO)_{sym}$) and their intensities increased with Pd loading. This result indicates that the characteristic trimeric structure of Pd(II) acetate was not preserved in the catalysts. The value of Δ_ν for the catalysts was between 95 and 124 cm^{-1}, which can be ascribed to the presence of the bidentate acetate (Δ_ν = 100 cm^{-1}) [38] or acetate group bridging two Ti atoms of the support (Δ_ν around 110–155 cm^{-1}) [40]. To confirm the possibility of formation of similar acetate species in our catalysts prepared by adsorption of $Pd(OAc)_2$ on hydrogen titanate nanotubes, we recorded the FT-IR spectrum of acetic acid impregnated on the NT support (Fig. S4B, Supporting Information). In this spectrum two bands were observed at 1545 and 1450 cm^{-1}, similar to those detected in the IR spectra of Pd(2.5)/NT and Pd(5.0)/NT catalysts (Fig. 6A). It seems that in the catalysts, these acetate species are in direct interaction with the nanotubular support. An increase in the Pd loading in the catalysts (Pd(7.5)/NT and Pd (10)/NT samples) resulted in the appearance of the secondary asymmetric and symmetric stretches at 1555 cm^{-1} and 1431 cm^{-1}, respectively, which indicates that in these catalysts, a new coordination mode of carboxylate binding appeared. Since the intensity of these bands increases with the palladium loading in the catalysts, it seems reasonable to assume that they correspond to some bidentate acetate in coordination with Pd species, such as Pd acetate dimer (with two bidentate acetate ligands coordinated to one central Pd ion) or terminal Pd bidentate acetate species. Therefore, the above results showed that the $Pd(OAc)_2$ trimer did not remain intact upon adsorption on the NT surface and suffered some decomposition due to a strong interaction with the support. In addition, the characteristics of the adsorbed acetate species changed depending on the palladium loading in the catalysts.

The FT-Raman spectrum of the $Pd(OAc)_2$ precursor is shown in Fig. S5 (inset) in the Supporting Information. This spectrum is well in line with a previous report for a palladium acetate trimer crystal where the most striking aspect was the strong vibration at 338 cm^{-1} assigned to a Pd acetate breathing mode, whereby acetate ligands stretch against Pd ions (ν(Pd-OAc) in phase vibrations) [38]. The strength of this band was attributed to a high conventional Raman polarizability. In the Raman spectra of the Pd(x)/NT catalysts (Fig. S5), the above signal was not observed, which once again confirms that the precursor's Pd(II) acetate structure was modified upon adsorption on the NT surface. In the 100–000 cm^{-1} region of the spectra, only four bands were observed at 190, 269, 454, and 658 cm^{-1} which are characteristic of the hydrogen form of titanate nanotubes [41].

The XPS analysis of Pd was performed to inquire into its chemical state in the prepared Pd(x)/NT catalysts with different metal loadings. The Pd3d spectrum of the starting Pd(II) acetate precursor is also shown for comparison (Fig. 7a). For palladium acetate, two peaks related to the spin–orbital doublet can be observed at 338.1 and 343.5 eV, corresponding to Pd3$d_{5/2}$ and Pd 3$d_{3/2}$, respectively. Fig. 7b and c shows the Pd3d regions of the Pd(5.0)/NT and Pd(10)/NT catalysts. In the spectrum of the first catalyst, it can be clearly seen that the signals of Pd species were shifted to lower binding energies than those of the $Pd(OAc)_2$ precursor. The spectrum b can be deconvoluted into two components with Pd3$d_{5/2}$ binding energies of 335.1 and 336.3 eV, which can be ascribed to Pd(0) and Pd(II) in PdO, respectively. Regarding the spectrum of the Pd(10)/NT catalyst with the highest palladium loading, three components are present in the Pd3$d_{5/2}$ region. Thus, in addition to the above-mentioned signals at 335.1 and 336.3 eV, a signal at 338.3 eV can be observed, indicating the presence of Pd(II) acetate-like species. The relative proportions of different types of Pd species in the catalysts with different Pd contents is shown in Table 2. It can be seen that at low Pd loading (5 wt.% of Pd $(OAc)_2$), Pd(II) as in PdO is predominant (77%), followed by reduced Pd(0). An increase in the palladium loading (Pd(10)/NT catalyst) resulted in the appearance of a small amount of Pd(II), similar to that in Pd(II) acetate, and in an increase in the proportion of reduced Pd(0) to 58%. These results are in line with a previous publication [26], where a similar increase in the proportion of Pd(0) species was observed with an increase in the bulk Pd content in the catalysts supported on titanate nanotubes and was attributed to the fact that the Pd clusters were becoming more metallic at higher loadings.

Summarizing the above FT-IR, FT-Raman, and XPS characterization results, it can be concluded that different kinds of palladium and acetate species are present in the Pd(x)/NT catalysts with different Pd loadings. It seems that at low Pd loadings (2.5 and 5.0 wt.% of $Pd(OAc)_2$), the precursor salt is decomposed upon adsorption, leading to the presence of acetate species in interaction with the

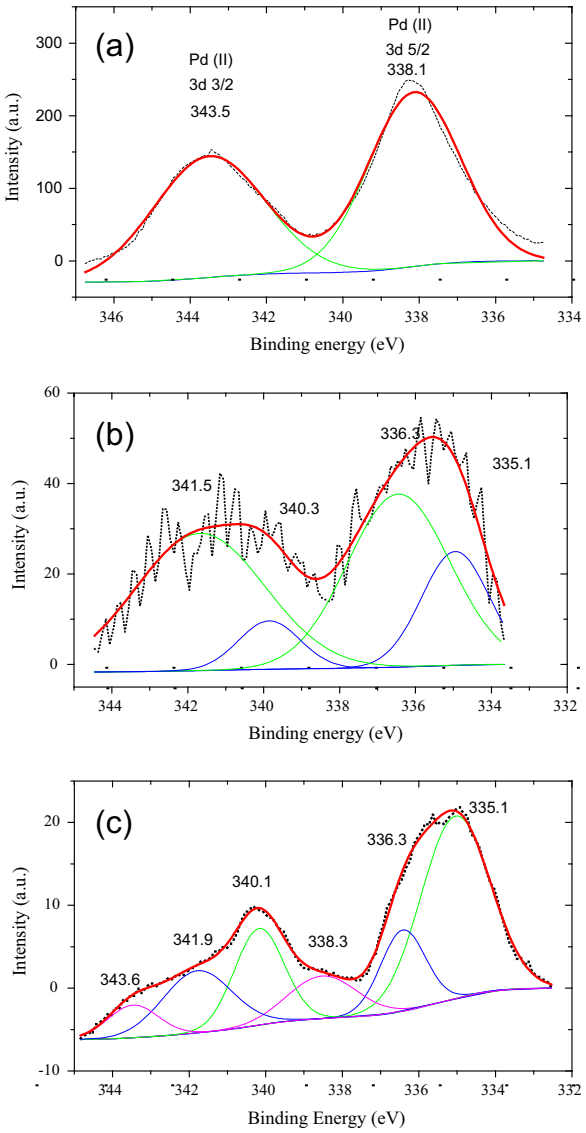

Fig. 7. XPS spectra of (a) $Pd(OAc)_2$ used as a precursor and of (b) Pd(5.0)/NT and (c) Pd(10)/NT catalysts.

Table 2
Binding energy (BE) and population of palladium species in different chemical states for the selected fresh and used Pd(*x*)/NT catalysts.

Sample	BE Pd $3d_{5/2}$ (eV)		
	Pd^{2+} in $Pd(OAc)_2$	Pd^{2+} in PdO	Pd^0
$Pd(OAc)_2$ precursor	338.1 (100%)	–	–
Fresh catalysts			
Pd(5.0)/NT	–	336.3 (77%)	335.1 (23%)
Pd(10)/NT	338.3 (15%)	336.3 (27%)	335.1 (58%)
Used catalysts[a]			
Pd(5.0)/NT (3C)		336.9 (47%)	335.0 (53%)
Pd(10)/NT (1C)			335.4 (100%)

[a] Catalysts used in one (1C) or three (3C) catalytic cycles.

nanotubular titanate support, whereas palladium is present as Pd (II) in PdO (major proportion) and reduced Pd(0). At high Pd contents, the presence of some bidentate acetate species in coordination with Pd(II) was observed by FT-IR, which was confirmed by XPS of the Pd3*d* region. The existence of these species was not detected by FT-Raman spectroscopy, probably because of their low population (15%) in comparison with other types of Pd species or due to the fact that these Pd-acetate species are different from those in the $Pd(OAc)_2$ trimer used as a precursor, which leads to the disappearance of the characteristic vibration at 338 cm^{-1}. In addition, it was observed that Pd(0) was present in all catalysts and its proportion increased with Pd loading. No additional reduction treatment was applied to our catalysts after drying, which indicates that the palladium reduction occurred during catalyst preparation. Previously, it was reported that acetate itself or water can function as reductants [42,43]. According to previous reports, there are a number of factors (Pd dispersion, Pd distribution, its oxidation state, water content in the catalysts, etc.) that affect catalytic activity and stability of heterogeneous Pd catalysts in Heck reactions. Therefore, the above differences in the characteristics of the prepared Pd(*x*)/NT catalysts led us to expect different catalytic performance in the selected Heck reactions.

3.2. Catalytic activity

Palladium catalysts prepared in the present work were tested in the Heck cross-coupling reaction of styrene and two aryl halides: 4-bromobenzaldehyde and 4-bromostyrene (Scheme 1). The structure of compounds 3 and 5 was confirmed by ^1H and ^{13}C NMR, IR spectroscopy, mass spectrometry, and elemental analysis (Fig. S6 and product characterization results in the Supporting Information).

The catalytic activity results and reaction conditions (reaction time and amount of catalyst used) are summarized in Table 3. A comparison was made with unsupported $Pd(OAc)_2$, used frequently as a catalyst for Heck reactions. It can be seen that all tested catalysts were active for the Heck reaction of styrene and 4-bromobenzaldehyde (4-BrBA) or 4-bromostyrene (4-BrST). The corresponding cross-coupled products were separated quantitatively, purified, and characterized. It was found that only the E-isomers of compounds 3 and 5 were obtained. The amount of the pure E-product finally obtained was used to calculate product yield in each reaction. It can be seen in Table 3 that the reaction between styrene and 4-bromobenzaldehyde performed with 0.49 mol.% of palladium(II) acetate in solution resulted in 79% product yield at reaction time 24 h. The turnover number (TON) calculated for $Pd(OAc)_2$ in the above reaction was 159. When the same reaction was performed using the Pd(*x*)/NT catalysts, product 3 yields between 43% (Pd(2.5)/NT) and 98% (Pd(10)/NT) were obtained. As expected, an increase in the product yield was obtained with an increase in the Pd loading in the catalysts. It is worth mentioning that in the experiments with the supported Pd (*x*)/NT catalysts, the amount of Pd varied between 0.15 and 0.04 mol.%, which was 3–12 times less than in the reference reaction performed with the dissolved $Pd(OAc)_2$ mentioned above. Therefore, it was possible to obtain high product yields using Pd (*x*)/NT catalysts containing a smaller amount of Pd.

TON values obtained for the Pd(*x*)/NT catalysts varied between 1037 and 675, decreasing with increased Pd loading, which can be attributed to some agglomeration of Pd species. In order to compare the efficiency of Pd catalysts in the supported and dissolved forms, an additional experiment was done using the same amount of dissolved $Pd(OAc)_2$ as in the Pd(5.0)/NT catalyst (0.08 mol.%). A product yield of 37% was obtained in this case (TON equal to 450 vs. 827 for the Pd(5.0)/NT supported catalyst). It is noteworthy that in the coupling of 4-bromobenzaldehyde with styrene under identical reaction conditions, TON values obtained for all Pd catalysts supported on NT were higher than those obtained for dissolved Pd(II) acetate, which demonstrates the higher efficiency of the supported catalysts in comparison with unsupported $Pd(OAc)_2$.

To inquire into the effect of the reaction time, an additional experiment was performed with the Pd(7.5)/NT catalyst, reducing

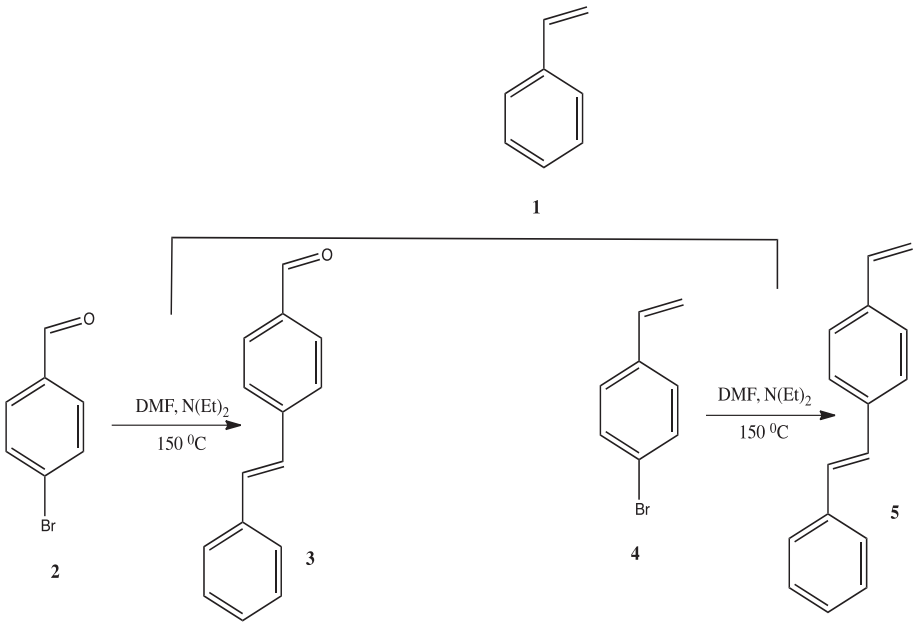

Scheme 1. Synthesis of (*E*)-4-styrylbenzaldehyde 3 and (*E*)-1-styryl-4-vinylbenzene 5.

Table 3
Catalytic activity of Pd catalysts in Heck coupling reactions of styrene with aryl halides.[a]

Catalyst	ArX[b]	Reaction time (h)	Amount of catalyst				Product yield (%)[c]	TON[d]
			Catalyst (mg)	$Pd(OAc)_2$ (mg)	Pd (mol.%)	Pd (mmol)		
$Pd(OAc)_2$	4-BrBA	24	15	15	0.49	0.067	79	159
$Pd(OAc)_2$	4-BrBA	24	2.5	2.5	0.08	0.011	37	450
Pd(2.5)/NT	4-BrBA	24	50	1.3	0.04	0.006	43	1037
Pd(5.0)/NT	4-BrBA	24	50	2.5	0.08	0.011	68	827
Pd(7.5)/NT	4-BrBA	24	50	3.7	0.12	0.017	96	785
Pd(7.5)/NT	4-BrBA	3	50	3.7	0.12	0.017	94	769
Pd(10)/NT	4-BrBA	24	50	4.4	0.15	0.020	98	675
Pd(10)/NT[e]	4-BrBA	0.75	25	10	0.14	0.010	29	206
Pd(5.0)/NTc	4-BrBA	24	50	2.5	0.08	0.011	64	778
Pd(5.0)/NTc	4-BrST	18	50	2.5	0.08	0.011	80	973
Pd(10)/NTc	4-BrBA	24	50	4.3	0.15	0.020	100	692

[a] All reactions were carried out under nitrogen at 150 °C using aryl halide (13.5 mmol), styrene (13.5 mmol), triethylamine (72 mmol), dimethylformamide (25 mL), and tri-(o-tolyl)phosphine (TOP, 1.64 mmol). The catalyst used, its amount, and the reaction time are shown in the table.
[b] ArX, aryl halide substrate: 4-BrBA, 4-bromobenzaldehyde; 4-BrST, 4-bromostyrene.
[c] Product yield was determined on the basis of the amount of coupling product separated and purified by column chromatography as (mol of coupling product)/(mol of used reactant). Only *E*-isomers of coupling products were obtained in all cases.
[d] TON = (mol of product)/(mol of catalyst).
[e] Reaction performed without TOP addition.

the reaction time from 24 to 3 h. Only a small decrease in the product yield (from 96% to 94%) was obtained, showing that it is possible to obtain high yields of product 3 at shorter times.

Water content in the supported Pd/C catalysts was also mentioned as an important factor that has a strong influence on catalytic activity in Heck coupling of bromobenzene with styrene [43]. TGA analysis of the NT support used for the preparation of a series of Pd(*x*)/NT catalysts with different metal loadings showed that it had high water content (about 17.1 wt.%). To decrease this content, a sample of the NT support was calcined at 350 °C for 2 h prior to catalyst preparation. The support obtained after this thermal treatment (labeled as NTc) contained about 4.8 wt.% of water and showed slightly increased textural characteristics (S_{BET}, V_P, and D_P) relative to the starting NT support (Table 1). Evaluation of the Pd(5.0)/NTc catalyst in the Heck reaction showed a yield of the product 3 (64%) similar to that obtained previously with the Pd(5.0)/NT sample and 80% yield in the coupling of 4-bromostyrene with styrene (product 5). The Pd(10)/NTc catalyst gave 100% yield of the product 3 at 24 h reaction time, whereas 98% yield was obtained with the corresponding Pd(10)/NT sample. Therefore, catalytic activity of the Pd catalysts with similar Pd loadings supported on uncalcined (NT) and calcined (NTc) materials was found to be similar in the first catalytic cycle.

Finally, according to the mechanism proposed by Heck for cross-coupling reactions of aryl halides and alkenes, Pd(0) is the catalytically active species. This species can be formed from of Pd $(OAc)_2$ with the help of monophosphine ligands (Pd^0L_n species) [44], where L can be, for example, tri-(o-tolyl)phosphine (TOP), used in the present work. In the case of heterogeneously catalyzed reactions, reduction can be performed with hydrogen gas [9,45], aqueous $NaBH_4$ solution [26], or other reduction agents. XPS results obtained for the Pd(*x*)/NT catalysts showed that all freshly prepared samples had some amount of the reduced Pd(0) species (Table 2). In order to inquire into the possibility of catalyzing the

Heck reaction using these Pd(0) species, an additional experiment was performed in the absence of TOP (Table 3, entry 8), obtaining 29% yield of the product 3 at 0.75 h reaction time. After that time, the catalyst turned black and lost activity.

3.3. Characterization of the used catalysts and their reutilization

After the catalytic activity tests, supported Pd catalysts were separated from the reaction mixture by filtration. This easy separation offers the possibility of reutilization of the catalysts in several catalytic cycles and quantitative recovery of palladium. It was observed that Pd(x)/NT catalysts with high Pd loadings (x = 7.5 and 10) changed their color to black due to the precipitation of catalytically inactive Pd black, whereas Pd(2.5)/NT, Pd(5.0)/NT, and Pd (5.0)/NTc did not change their color (Fig. 8).

Formation of large (15–35 nm) metallic Pd particles in the used Pd(10)/NT catalyst was also confirmed by powder XRD (Fig. 9A) and TEM (Fig. 10). In addition, in the Pd(10)/NT (1C) sample, a small signal at about 18° (2θ) was observed, evidencing the formation of black titanium oxide with the formula Ti_3O_5, which indicates that the NT support also suffered some changes during the reaction. The XPS characterization of the Pd(10)/NT catalyst after one reaction cycle showed only the presence of Pd(0) (Fig. 11 and Table 2).

Since only the catalysts with low palladium loadings maintained their light brown color after the reaction, we tested the possibility of recycling and reusing two of them: Pd(5.0)/NT and Pd (5.0)/NTc. These selected catalysts had similar Pd loadings (around 5 wt.% of $Pd(OAc)_2$, Table 1), the difference between them being in the amount of water in the support (17.1 wt.% in NT and 4.8 wt.% in NTc) and their textural characteristics (Table 1). Results obtained with these catalysts in recycling studies are shown in Table 4. After each catalytic activity test, recovered catalyst was washed with dichloromethane and dried in vacuum.

It can be seen in Table 4 that when the recycled Pd(5.0)/NT catalyst was used for the second and third times, a noticeable decrease in the product yield took place (from about 68% to 26% and 13%, respectively). After three cycles, the catalyst maintained its light brown color. No formation of Pd black was detected by XRD and HRTEM. However, some agglomeration of the deposited palladium species cannot be excluded. In addition, an increase in the proportion of Pd(0) in the twice reused Pd(5.0)/NT catalyst was detected by XPS (Fig. 11a and Table 2). The above could be the main reasons for deactivation of the Pd catalysts supported on NT material [26,42,43]. XRD characterization of the used Pd (5.0)/NT catalyst showed that some Ti_3O_5 was formed in the NT support after three catalytic cycles (Fig. 9A). The Pd(5.0) catalyst supported on the NTc material with lower water content (4.8 wt. %) showed almost stable catalytic activity in five catalytic cycles (Table 4). Only a slight decrease in the product yield was observed in the third and fourth recycles of the same catalyst, which can be ascribed to a loss of catalyst during filtration. No formation of any Pd black or crystalline Ti_3O_5 was found in this case (Fig. 9B). We attribute this behavior to lower water content in the calcined nanotubular support. It is known that nanotubular titanate materials contain a significant amount of water with different characteristics: physisorbed and chemisorbed (interlayer and structural) water [33]. Calcination of NT material at 350 °C for 2 h results in the elimination of most of the physisorbed and part of the chemisorbed (interlayer) water, whereas structural water remains in the nanotubes. Our results show that an excess of water in the nanotubular titanate support has a negative effect on the catalytic activity of recycled catalysts; meanwhile, the presence of a small amount of structural water is necessary for the stabilization of Pd catalysts. In order to prove the above supposition, a reference Pd(5.0)/TiO_2 catalyst was prepared using commercial titania nanopowder as a support. This catalyst did not have any water content. Activity evaluation in the reaction of 4-bromobenzaldehyde with styrene showed high product 3 yield (71% under the same reaction conditions as in Table 4). However, the catalyst separated after the reaction became completely black, so its recycling was not possible.

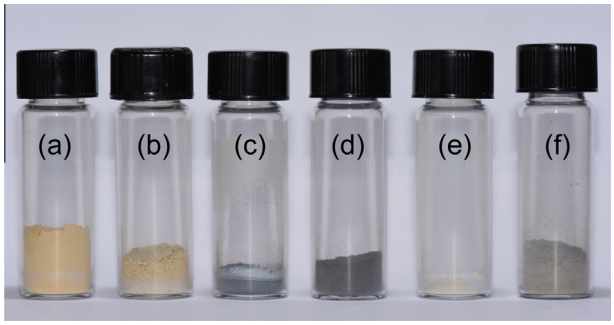

Fig. 8. Catalysts after one catalytic cycle: (a) Pd(2.5)/NT, (b) Pd(5.0)/NT, (c) Pd(7.5)/NT, and (d) Pd(10)/NT. Used catalysts supported on calcined NTc material: (e) Pd (5.0)/NTc after five catalytic cycles and (f) Pd(10)/NTc after three catalytic cycles. Catalysts with low palladium loading (x = 2.5 and 5.0) maintained their color after the Heck reaction, whereas catalysts with high palladium loading turned black or gray.

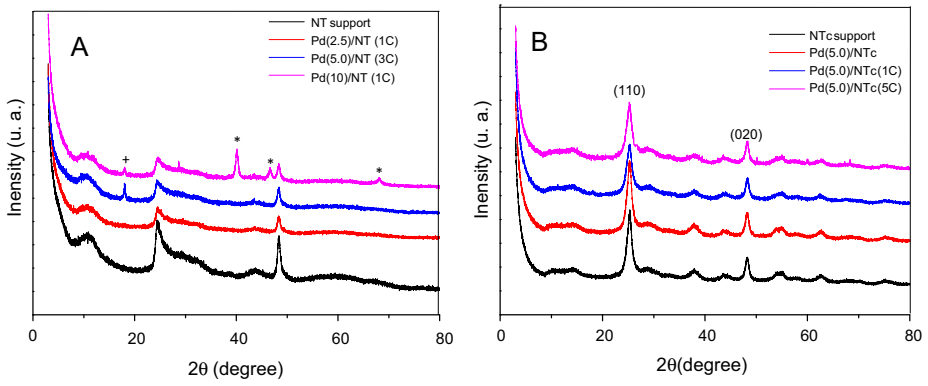

Fig. 9. (A) XRD patterns of Pd(x)/NT catalysts after one (1C) or three (3C) catalytic cycles. * Palladium, syn. (ICDD card 00-005-0681); + titanium oxide Ti_3O_5 (ICDD card 04-007-6635). (B) XRD patterns of fresh Pd(5.0)/NTc catalyst and after one (1C) or five (5C) catalytic cycles. (1 1 0) and (0 2 0) reflections of the hydrogen trititanate phase $H_2Ti_3O_7$ (JCPDS-ICDD card 47-0561) of the NTc support are indicated.

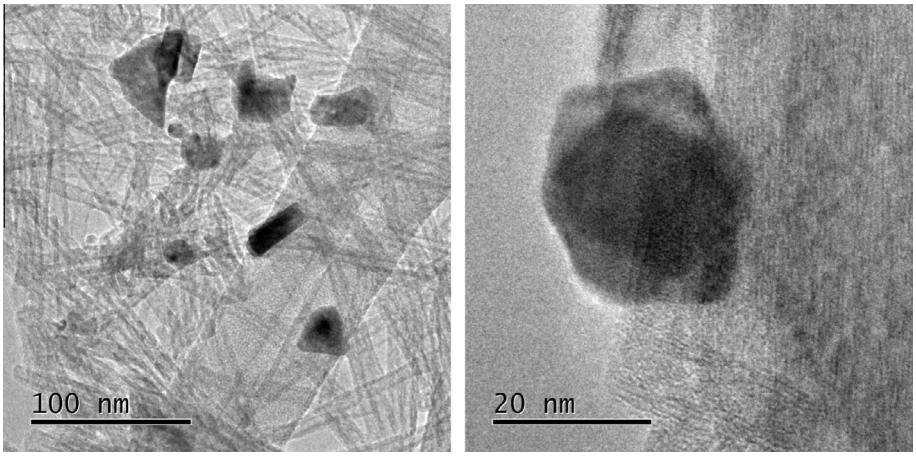

Fig. 10. TEM images of the Pd(10)/NT catalyst after one catalytic cycle. Dark particles of Pd black can be observed.

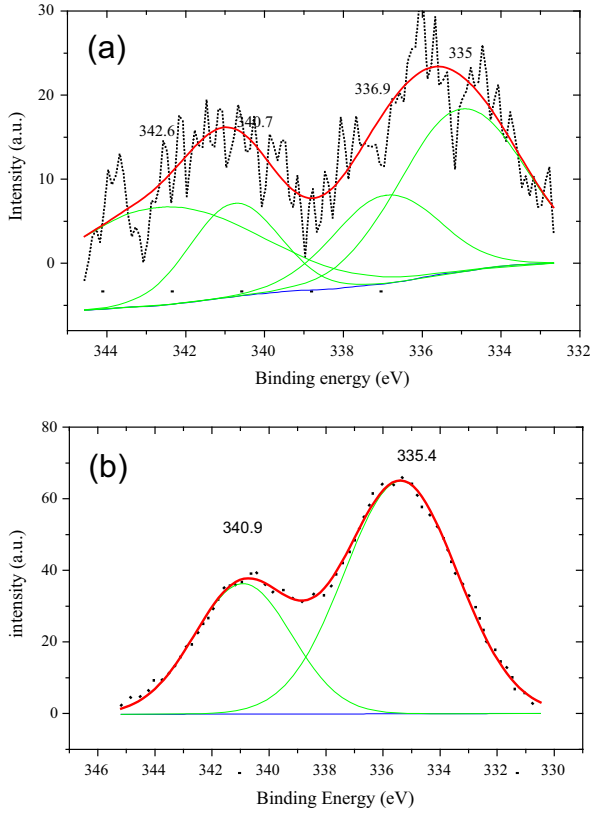

Fig. 11. XPS spectra of (a) Pd(5.0)/NT catalyst after three catalytic cycles (3C) and (b) Pd(10)/NT catalyst after one catalytic cycle (1C).

To inquire into the stability of the high-loading Pd catalysts supported on calcined NTc material, the Pd(10)/NTc sample was prepared and tested in recycling studies. This catalyst showed high activity in the first catalytic test (100% product 3 yield at 24 h, Table 3). However, its activity significantly decreased in the next cycles (Table 4). In addition, the color of this catalyst changed to gray after three catalytic cycles (Fig. 8f). Nevertheless, a comparison of the deactivation processes of Pd(10)/NT and Pd(10)/NTc samples shows that deactivation of the Pd(10) catalyst supported on calcined NTc material was much slower than that of the NT-supported analog, which deactivated completely after the first catalytic test (see Fig. 8d). This result once again shows that calcination of the NT support delays the process of agglomeration of Pd species and formation of Pd black. Finally, from the above experiments, it can be concluded that low Pd loading (up to 5 wt.% of $Pd(OAc)_2$) and the presence of a small amount of structural water (about 5 wt.%) in the nanotubular support are the factors that provide stability to the supported Pd catalysts, opening up the possibility of their recycling and reutilization.

Table 4
Re-use of Pd catalysts supported on NT and NTc materials in Heck coupling of 4-bromobenzaldehyde with styrene.[a]

Catalyst	Product **3** yield (%)				
	Fresh catalyst	1st reuse	2nd reuse	3rd reuse	4th reuse
Pd(5.0)/NT	68	26	13	–	–
Pd(5.0)/NTc	64	62	64	53	56
Pd(10)/NTc	100	65	21	–	–

[a] Reaction conditions: nitrogen atmosphere, temperature 150 °C, 4-bromobenzaldehyde (13.5 mmol), styrene (13.5 mmol), triethylamine (72 mmol), dimethylformamide (25 mL), and tri-(o-tolyl)phosphine (TOP, 1.64 mmol), 0.05 g of the catalyst, 24 h reaction time.

4. Discussion

Nowadays, the development of active and stable heterogeneous Pd catalysts for the Heck reaction is an actual task. These catalysts have the advantage of easy separation from the reaction mixture and therefore can be reused if they are not deactivated. Many attempts have been made recently to find an appropriate catalytic system. In many cases, highly active catalysts were obtained; however, their stability was not as good as desired. For example, in work [43], Pd catalysts supported on activated carbon (Pd/C) were used for Heck coupling of bromobenzene with styrene. The optimization of the catalyst and reaction conditions allowed Pd/C catalysts with very high activity in the above reaction (TON ≈ 18,000). However, the dramatic decrease in Pd dispersion during the reaction resulted in a significant decrease in catalytic activity. Thus, the conversion decreased from 92% (new catalyst) to 63% in the first reuse and to 4% in the second reuse. Characterization of the Pd/C catalyst before and after the reaction by TEM showed agglomeration of the Pd species after the reaction. In work [9], Heck olefination of aryl halides over Pd-TMS11 catalysts prepared by palladium grafting on the Nb-MCM-41 material was studied. The Pd-TMS11 catalyst recovered after three catalytic cycles in the reaction between *n*-butyl acrylate and 1-bromo-4-nitrobenzene,

with a total TON of 3000, showed in the XRD pattern some agglomeration of palladium, evidenced by two peaks of palladium between $2\theta = 40°$ and 50°. In work [26], Pd catalysts supported on titanate nanotubes were used for double-bond migration in allylbenzene. In all reactions, the orange-brown catalysts became completely black within the first 5 min. From the above examples, it is clear that agglomeration of palladium species and formation of Pd black are the main reasons for the deactivation of heterogeneous palladium catalysts. Similarly, formation of Pd black is a well-known phenomenon for homogeneously catalyzed Heck reactions [42]. Different approaches were used in homogeneous and heterogeneous catalysis to stabilize Pd species against agglomeration. In the present work, we tried to reach this aim by using strong metal–support interaction between Pd species and the nanotubular hydrogen titanate support.

Following this idea, we selected the adsorption of Pd(II) acetate on the support surface as the catalyst's preparation method. This would ensure the presence in the catalysts of only Pd species in interaction with the titanate support. A variety of Pd(x)/NT catalysts with different Pd loadings supported on NT material were prepared. Catalytic activity tests and recycling experiments showed that catalysts with low Pd loading ($x = 2.5$ and 5.0) were more active (had higher TON values) and more stable than the high-Pd-loading ones. This could be ascribed to good dispersion and homogeneous distribution of Pd species in them. Further elimination of physisorbed and interlayer water from titanate nanotubes by calcination resulted in the Pd(5.0)/NTc catalyst, which showed almost constant catalytic activity in five catalytic cycles. Therefore, we think that the proposed approach to stabilization of Pd catalysts by metal–support interaction led to good results. Strong metal–support interaction in the catalysts with low Pd loadings (up to 5 wt.% Pd(II) acetate) was confirmed by the fact that the starting $Pd(OAc)_2$ precursor was decomposed after adsorption into Pd(II) species as PdO and Pd(0), whereas the acetate group was coordinated to the Ti atoms of the support. In the high-loading fresh Pd(10)/NT catalyst, in addition to Pd(II)O and Pd(0), some Pd (II) species, as in $Pd(OAc)_2$, were detected with an increase in the proportion of reduced Pd(0). This catalyst showed a low TON value, as well as low stability. This result is in line with previous observations [43], where high activity in the Heck coupling of bromobenzene with styrene was shown by catalysts with a low degree of Pd reduction. According to our results, an increase in the proportion of Pd(0) also has a negative effect on catalytic activity and stability, since it promotes the formation of Pd black and increases the rate of deactivation.

Regarding the mechanism of the homogeneous Heck reaction [44], it is generally considered that $Pd(0)L_n$ is a catalytically active entity and the reaction starts by oxidative addition of aryl halide (ArX) to Pd(0), which changes its oxidation state to 2+. When aryl bromides are used, their oxidative addition to Pd(0) is slow and this first step of the catalytic cycle becomes the rate-determining step. As a consequence, most of the palladium is present in the form of Pd(0), and if its concentration increases, agglomeration of Pd(0) occurs faster, leading to the formation of palladium black and the Heck reaction stops. Recently, it was proposed that when heterogeneous Pd catalysts are used in the Heck reactions performed at high temperature (120–160 °C) [42,43,46], leaching of Pd species into the solution occurs during the reaction, and that these dissolved Pd species function as a highly active homogeneous catalyst in the Heck reaction. However, after the reaction was finished, less than 1 ppm of palladium was found in the solution, indicating that active palladium species reprecipitated onto the support's surface. Therefore, it was proposed that the solid catalyst functions as a source of molecular palladium species in solution. Previously, the above behavior was observed for Pd catalysts supported on different materials: carbon [43], titania, alumina, and NaY zeolite [46]. In order to confirm that similar Pd leaching could have taken place in the case of our catalysts supported on nanotubular titanate in the Heck reaction between 4-bromobenzaldehyde and styrene at 150 °C, an additional experiment was performed with the Pd(10)/NT catalyst. In this experiment, samples of the reaction solution and the catalyst were withdrawn at 30 min reaction time (after reaching a temperature of 150 °C) and analyzed. The catalyst's analysis by SEM-EDX showed about a 30–37% decrease in the palladium loading. On the other hand, chemical analysis of the filtered and evaporated sample of the reaction solution (3 mL) by atomic absorption spectroscopy (AAS) showed the presence of palladium in the residue. The amount of Pd in the reaction solution was estimated to be about 20–22 ppm. The above results confirmed the possibility of leaching of part of the Pd contained in the Pd(10)/NT catalyst into the solution during the reaction. However, it was not clear if this leaching was irreversible or the leached Pd species were readsorbed back onto the NT support's surface. To answer this question, we determined the Pd content in the catalysts of the Pd(x)/NT series shown in Fig. 8a–d after use in one catalytic cycle. In all cases, the Pd loading in the used catalysts was similar to that in the fresh samples. For example, the Pd(10)/NT catalyst separated after the end of the reaction (24 h reaction time) showed a Pd content corresponding to 8.47 wt.% as $Pd(OAc)_2$, which is very close to the Pd loading in the fresh catalyst (8.84 wt.%, Table 1). The above result indicates that all Pd species leached from the Pd(10)/NT catalyst during the reaction were redeposited onto the NT surface when the reaction finished. Therefore, the possibility of irreversible palladium leaching during the reaction could not be considered as a possible cause of deactivation. In addition, the reaction product 3, separated after the end of the reaction, was tested for the presence of Pd, giving a negative result. The above observations are well in line with previously mentioned reports [43,46] and point out the possibility of Pd leaching into the reaction solution during the reaction and its redeposition onto the titanate support.

Regarding the product inhibition as another possible cause for the deactivation of the Pd(x)/NT catalysts, we tested for the presence of the product 3 in the used catalysts, shown in Figs. 8a–d. Since product 3 has a large conjugated system of π bonds, it is a highly fluorescent compound upon UV irradiation. No fluorescence was detected in the used Pd(x)/NT catalysts when they were exposed to UV light (333 nm). From the above, it seems that the main reason for the deactivation of the studied Pd catalysts supported on hydrogen titanate nanotubes was agglomeration of Pd species and formation of Pd black.

The explanation for the quick deactivation of the Pd(x)/NT catalysts with high Pd loadings should be related to the amount of Pd leached from the solid catalyst into the solution. This amount should be larger at high Pd loading in the Pd(x)/NT catalysts ($x = 7.5$ and 10), as well as due to the presence in these catalysts of some reversibly adsorbed $Pd(OAc)_2$-like species (part II of the Pd acetate adsorption isotherm, Fig. 2) in weak interaction with the support. An increase in the concentration of Pd species leached into solution would accelerate the agglomeration of the Pd species and the formation of Pd black. On the other hand, the stability of the low-Pd-loading Pd(x)/NT catalysts could be due to the strong interaction of the adsorbed Pd with the NT support and the low proportion of Pd(0), both of which diminish the amount of leached Pd(0) in the solution, decreasing Pd agglomeration and deactivation of the catalyst. In addition, the nanotubular titanate support can also facilitate back precipitation of the reduced Pd(0) from the solution and promote reoxidation of Pd(0) to Pd(II), which was evidenced by the formation of the reduced Ti_3O_5 oxide (Fig. 9A). Therefore, we consider that the participation of the nanotubular support in the stabilization of Pd^{2+} species on its surface can be important for preventing the formation of Pd black and cat-

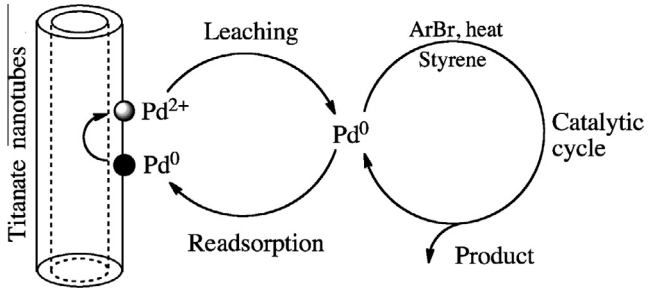

Scheme 2. Proposed mechanism for the action of the stable Pd(5.0)/NTc catalyst. Palladium species participate in two cycles: (1) leaching of Pd^{2+} from the NTc support into the solution and readsorption and (2) the Heck reaction catalytic cycle taking place in the solution.

alyst deactivation. Finally, the amount of water in the nanotubular hydrogen titanate is another important factor in the stability of the supported Pd catalysts, the presence of a large amount of physisorbed and interlayer water being undesired. Possibly, the presence of an excessive amount of water in the catalyst promotes the reduction of Pd(II) species to Pd(0) which can be further transformed into Pd black.

Results obtained in the present work show that both support properties (water content) and Pd loading are important for the stability of Pd catalysts supported on hydrogen titanate nanotubes. In addition, the possibility of Pd leaching and readsorption during the Heck reaction was proved. From the above results and considering that the main reason of the Pd catalysts' deactivation is the formation of Pd black, a possible reaction mechanism can be proposed (Scheme 2). In this mechanism, the Heck reaction catalytic cycle took place in the solution with the participation of Pd leached from the solid catalyst. After leaching, dissolved Pd species can be readsorbed again on the nanotubular support, and it seems that the role of the support is to maintain a correct balance between Pd(0) and Pd(II) species, to stabilize the catalyst and prevent an increase in the proportion of reduced Pd(0) species, leading to the formation of Pd black. To keep the catalyst stable, both cycles should work together to maintain a small concentration of Pd species in the reaction solution, thus preventing their agglomeration and the precipitation of Pd black. In addition, the higher catalytic activity of the Pd catalysts supported on titanate nanotubes than of pure Pd (II) acetate under homogeneous catalysis conditions indicates that Pd species leached from the catalysts supported on titanate nanotubes are more active than those obtained from $Pd(OAc)_2$ or that Pd species deposited on the support's surface (nonleached) can also be highly active for catalyzing the Heck reaction. However, these assumptions need further experimental confirmation and a more detailed reaction mechanism and kinetic study.

5. Conclusions

In the present work, Pd catalysts supported on hydrogen titanate nanotubes were synthesized and characterized. It was found that the deposited Pd species were well-dispersed and homogeneously distributed in all catalysts. The oxidation state of the supported Pd species depended on the Pd loading. In general, three types of Pd were found in the catalysts, namely, Pd(II) in PdO and Pd(0) at low Pd loadings (up to 5 wt.% of Pd(II) acetate) and some Pd(II) in the $Pd(OAc)_2$-like species at a higher Pd loading. The effect of the water content in the titania nanotubes was also tested. The Pd(5.0)/NTc catalyst containing about 5 wt.% of water was found to be surprisingly stable, maintaining almost constant activity in the Heck reaction of 4-bromobenzaldehyde and styrene after five catalytic cycles. The possible explanation for the catalyst's stability and deactivation through the formation of Pd black was proposed. It considers both the catalyst's Pd loading and the possibility of leaching of the Pd species into the reaction solution and their readsorption back, where the NT support helps to maintain a correct balance of different oxidation states of Pd, preventing the formation of Pd black.

Acknowledgments

Financial support from DGAPA-UNAM, Mexico (Project PAPIIT IN-113715) and CONACYT, Mexico (Project CB 220175), is gratefully acknowledged. The authors thank C. Salcedo Luna and I. Puente Lee for technical assistance with powder XRD and electron microscopy (SEM-EDX and HRTEM) characterizations, respectively. We are also grateful to Luis Escobar-Alarcón for help with FT-Raman characterization of the catalysts.

Appendix A. Supplementary material

Supplementary data associated with this article can be found, in the online version, at http://dx.doi.org/10.1016/j.jcat.2016.07.019.

References

[1] J. Tsuji, Palladium Reagent and Catalyst – Innovations in Organic Synthesis, Wiley, Chichester, UK, 1995.
[2] R.F. Heck, Palladium Reagents in Organic Synthesis, Academic Press, London, 1985.
[3] J. Tsuji, in: B.M. Trostand, I. Fleming (Eds.), Comprehensive Organic Synthesis, vol. 7, Pergamon Press, Oxford, 1991.
[4] A. de Meijere, F. Meier, Angew. Chem. 106 (1994) 2473.
[5] N. Arul Dhas, H. Cohen, A. Gedanken, J. Phys. Chem. B 101 (1997) 6834.
[6] M. Andersson, E. Bakchinova, K. Jansson, M. Nygren, J. Mater. Chem. 9 (1999) 265.
[7] A.A. Mastalir, L. Turi, Z. Kiraly, I. Dekany, M. Bartok, Mol. Cryst. Liq. Cryst. Sci. Technol. Sect. A 311 (1998) 333.
[8] D. Guillemot, M. Polisset-Thfoin, D. Bonnin, D. Bazin, J. Fraissard, J. Phys. IV 7 (1997) 931.
[9] C.P. Mehnert, D.W. Weaver, J.Y. Ying, J. Am. Chem. Soc. 120 (1998) 12289.
[10] G.M. Neelgund, A. Oki, Appl. Catal. A 399 (2011) 154.
[11] M. Zhao, R.M. Crooks, Angew. Chem. Int. Ed. 38 (1999) 364.
[12] A.B.R. Mayer, J.E. Mark, R.E. Morris, Polym. J. 30 (1998) 197.
[13] T. Kasuga, M. Hiramatsu, A. Hoson, T. Sekino, K. Niihara, Langmuir 14 (1998) 3160.
[14] X. Sun, Y. Li, Chem. Eur. J. 9 (2003) 2229.
[15] Z.Y. Yuan, B.L. Su, Colloids Surf. A Physicochem. Eng. Aspects 241 (2004) 173.
[16] C.C. Tsai, H. Teng, Chem. Mater. 16 (2004) 4352.
[17] C.H. Lin, S.H. Chien, J.H. Chao, C.Y. Sheu, Y.C. Cheng, Y.J. Huang, C.H. Tsai, Catal. Lett. 80 (2002) 153.
[18] V. Idakiev, Z.-Y. Yuan, T. Tabakova, B.-L. Su, Appl. Catal. A 281 (2005) 149.
[19] C.H. Lin, C.H. Lee, J.H. Chao, C.Y. Kuo, Y.C. Cheng, W.N. Huang, H.W. Chang, Y.M. Huang, M.K. Shih, Catal. Lett. 98 (2004) 61.
[20] J.C. Xua, M. Lua, X.Y. Guob, H.L. Lia, J. Mol. Catal. A 226 (2005) 123.
[21] J.J. Yang, Z.S. Jin, X.D. Wang, W. Li, J.W. Zhang, S.L. Zhang, X.Y. Guo, Z.J. Zhang, Dalton Trans. 20 (2003) 3898.
[22] D.V. Bavykin, V.N. Parmon, A.A. Lapkin, F.C. Walsh, J. Mater. Chem. 14 (2004) 3370.
[23] D.V. Bavykin, A.A. Lapkin, P.K. Plucinski, L. Torrente-Murciano, J.M. Friedrich, F. C. Walsh, Top. Catal. 39 (2006) 151.
[24] D.V. Bavykin, S.N. Gordeev, A.V. Moskalenko, A.A. Lapkin, F.C. Walsh, J. Phys. Chem. B 109 (2005) 8565.
[25] J. Hong, J. Cao, J. Sun, H. Li, H. Chen, M. Wang, Chem. Phys. Lett. 380 (2003) 366.
[26] L. Torrente-Murciano, A.A. Lapkin, D.V. Bavykin, F.C. Walsh, K. Wilson, J. Catal. 245 (2007) 272.
[27] S.K. Mohapatra, N. Kondamudi, S. Banerjee, M. Misra, Langmuir 24 (2008) 11276.
[28] R. Camposeco, S. Castillo, I. Mejía-Centeno, J. Navarrete, J. Marín, Mater. Char. 95 (2014) 201.
[29] C.-H. Han, D.-W. Hong, I.-J. Kim, J. Gwak, S.-D. Han, K.C. Singh, Sens. Actuat. B 128 (2007) 320.
[30] T. Kasuga, M. Hiramatsu, A. Hoson, T. Sekino, K. Niihara, Adv. Mater. 11 (1999) 1307.
[31] Q. Chen, G.H. Du, S. Zhang, L.-M. Peng, Acta Crystallogr. B 58 (2002) 587.
[32] R.A. Ortega-Domínguez, J.A. Mendoza-Nieto, P. Hernández-Hipólito, F. Garrido-Sánchez, J. Escobar-Aguilar, S.A.I. Barri, D. Chadwick, T.E. Klimova, J. Catal. 329 (2015) 457.
[33] E. Morgado Jr., M.A.S. de Abreu, G.T. Moure, B.A. Marinkovic, P.M. Jardim, A.S. Araujo, Chem. Mater. 19 (2007) 665.

[34] G. Leofanti, M. Padovan, G. Tozzola, B. Venturelly, Catal. Today 41 (1998) 207.
[35] C.K. Lee, K.-S. Lin, C.-F. Wu, M.-D. Lyu, C.-C. Lo, Hazard. Mater. 150 (2008) 494.
[36] S. Mozia, E. Borowiak-Palén, J. Przepiórski, B. Grzmil, T. Tsumura, M. Toyoda, J. Grzechulska-Damszel, A.W. Morawski, J. Phys. Chem. Solids 71 (2010) 263.
[37] A.J. Maira, J.M. Coronado, V. Augugliaro, K.L. Yeung, J.C. Conesa, J. Soria, J. Catal. 202 (2001) 413.
[38] D.D. Kragten, R.A. van Santen, M.K. Crawford, W.D. Provine, J.J. Lerou, Inorg. Chem. 38 (1999) 331.
[39] K. Ito, H.J. Bernstein, Canad. J. Chem. 34 (1956) 170.
[40] S. Doeuff, Y. Dromzee, F. Taulelle, C. Sanchez, Inorg. Chem. 28 (1989) 4439.
[41] A. Gajović, I. Friščić, M. Plodinec, D. Iveković, J. Mol. Struct. 924–926 (2009) 183.
[42] J.G. de Vries, Dalton Trans. (2006) 421.
[43] K. Köhler, R.G. Heidenreich, J.G.E. Krauter, J. Pietsch, Chem. Eur. J. 8 (2002) 622.
[44] H.A. Dieck, R.F. Heck, J. Am. Chem. Soc. 96 (1974) 1133.
[45] J.H. Ding, D.L. Gin, Chem. Mater. 12 (2000) 22.
[46] S.S. Pröckl, W. Kleist, M.A. Gruber, K. Köhler, Angew. Chem. Int. Ed. 43 (2004) 1881.